



Control of spatio-temporal variability of ocean nutrients in the East Australian Current

Megan Jeffers¹, Chis Chapman², Bernadette M. Sloyan², and Helen Bostock¹

¹School of the Environment, Faculty of Science, The University of Queensland, Australia

²CSIRO Environment, Hobart Marine Laboratories, Hobart, Australia

Correspondence: Megan Jeffers (m.jeffers@uq.edu.au)

Abstract. The East Australian Current (EAC), the South Pacific's southward flowing western boundary current, dominates the marine environment of the east coast of Australia. Upwelling of deep EAC nutrient rich water into the oligotrophic surface waters is very important for maintaining upper ocean productivity. However, the role of EAC dynamics in upper ocean nutrient variability and resulting productivity is poorly understood. In this study we use physical and biogeochemical data collected from 2012–2022 to improve understanding of the variability of the nutrients in the upper water column at $\sim 27^\circ$ S, a subtropical region strongly influenced by EAC.

The 10-year data set shows that there is a seasonal increase in nutrient concentrations in the upper water column (0–200 m) in the Austral spring (September–November) and autumn (March–May), and a minimum in winter (June–August). We also find that the nutrient concentrations in the upper water column are influenced by the position of the EAC jet. Two main modes of variability in the EAC's position are identified: an inshore mode with jet flowing along the continental slope and; an offshore mode with the current core detached from the continental slope and flowing over the adjacent abyssal plain. The position of the EAC jet influences the location of upwelling of nutrient-rich water at depth (>200 m). For the EAC inshore mode, cooler, nutrient-rich waters are restricted to the area of the continental shelf and slope that is inshore of the EAC. The offshore mode exhibits a wider distribution of nutrient-rich waters over both the inshore shelf and slope and, offshore abyssal Tasman Sea. Our analysis highlights the important interactions between nutrient concentrations and distribution and the highly variable EAC, which has implications for primary production, fisheries, and the biological carbon pump.

1 Introduction

The East Australian Current (EAC) is the western boundary current (WBC) of the South Pacific subtropical gyre, and plays a significant role in the southwest Pacific Ocean circulation and nutrient distribution. The EAC transports warm water from the Coral Sea into the Tasman Sea (Archer et al., 2017a; Sloyan et al., 2016). The upper EAC waters (0–200 m) are oligotrophic (low nutrient concentration), however below 200 m the EAC transports nutrient rich water southwards.

The EAC is fed by the South Equatorial Current via several westward flowing jets between 15° S and 23° S. The North Vanuatu and the North Caledonian jets flow into the northern Coral Sea at $\sim 15^\circ$ S and $\sim 19^\circ$ S, respectively, providing inflowing waters that are warm and salty, with low oxygen and nutrient concentrations (Kessler and Cravatte, 2013). At these



25 latitudes the EAC has a relatively weak southward transport of between 6–8 Sv (Ganachaud et al., 2014; Kessler and Cravatte, 2013). Around 23° S, the addition of the sub-surface South Caledonian Jet strengthens the EAC flow to a mean southward
30 transport of 24.6 Sv and also increases the subsurface oxygen concentrations (Kessler and Cravatte, 2013; Sloyan et al., 2016). This marks the start of the EAC jet “intensification zone” that extends southwards until the separation latitude at approximately 31–34° S (Oke et al., 2019; Ridgway and Dunn, 2003). At the separation latitude, the EAC bifurcates into two eddy-dominated
35 flow paths, with one proceeding southward along the eastern Australian coast to Tasmania known as the south EAC extension, and the other flowing across the Tasman Sea to New Zealand as the Tasman Front, or east EAC extension (Ganachaud et al., 2014; Godfrey et al., 1980; Oke et al., 2019; Ridgway and Dunn, 2003; Sutton and Bowen, 2014). However, recent work has shown that the latitude of the separation point is significantly influenced by changes in the EAC further upstream (Li et al., 2021), emphasising the importance of understanding the EAC jet further upstream.

40 Between the latitudes of 25–30° S the EAC, whilst maintaining a more coherent jet-like flow, is highly dynamic due to interactions with mesoscale eddies (Archer et al., 2017a; Oke et al., 2019) and larger scale forcing (Sloyan and O’Kane, 2015; Bull et al., 2020). This meandering of the jet can cause significant changes to the vertical structure of the current and southward transport (Roughan et al., 2022b; Sloyan et al., 2016). Previous work at ~27° S identified a meander in the EAC jet which shifted the position of the main poleward (southward) flow laterally, on and off the continental slope (Sloyan et al., 2016).

45 Additionally, the EAC exhibits seasonal changes in its physical flow. Several observational-based studies have revealed a seasonal change of approximately 9 Sv in the volume transport of the EAC, with the maximum occurring in austral summer and minimum in winter (Archer et al., 2017a; Godfrey et al., 1980; Ridgway and Godfrey, 1997). Temperature and salinity also show a seasonal cycle when considering the surface waters (potential density $\rho_0 > 26.2 \text{ kg/m}^3$), which are warmer and fresher during the summer (Oke et al., 2019).

50 Upwelling of deeper EAC nutrient rich water into the oligotrophic surface waters influences the primary production patterns, plankton community composition, and nutrient utilization strategies of marine organisms along the east coast of Australia (Everett et al., 2014; Hassler et al., 2011). At 29° S, Everett et al. (2014) identified a seasonal cycle in dissolved nutrients with increased dissolved nitrate and silicate concentrations in Austral winter and spring (June - September). Previous work has shown that the EAC separation point is characterized by upwelling, resulting in an enhanced nutrient supply and increased
55 biological activity, contributing to more productive fisheries (Everett et al., 2011; Figueira and Booth, 2010; Hassler et al., 2011; Olson, 2001; Suthers et al., 2023). The upwelling of the nutrients to the surface layer in this region has been attributed to various factors, including wind forcing, EAC divergence, and the presence of eddies (Everett et al., 2011; Gibbs et al., 1998; Godfrey et al., 1980; Rochford, 1975; Roughan and Middleton, 2002, 2004). Some studies attribute the increased nutrient supply to the higher velocity of the current induced by topographic forcing (Blackburn and Cresswell, 1993; Boland and Church, 1981; Oke and Middleton, 2000), while other studies attributed the increased nutrient concentrations to the action of the EAC separating from the coast (Tranter et al., 1986). At the separation point, it has been suggested that shifts in the position of the EAC are associated with periods of increased nutrient upwelling (Rochford, 1975), resulting in the transport of nutrient-rich waters onto the continental shelf and coastal (Everett et al., 2014; Oke and Middleton, 2001; Roughan and Middleton, 2004). Roughan and Middleton (2002) find that when the EAC shifted towards the coast, nutrient upwelling to the



60 surface occurred alongside uplifted isotherms. This upwelling supports considerable productivity in coastal and shelf regions in
an otherwise relatively low productivity region (Nieblas et al., 2009; Roughan et al., 2022a; Schaeffer et al., 2013). While there
is evidence that EAC dynamics influence nutrient supply to the euphotic upper ocean, our understanding of nutrient dynamics
within the EAC is limited, largely due to a lack of data (Everett et al., 2011, 2014; Hassler et al., 2011; McGillicuddy Jr, 2016;
Oke and Middleton, 2001; Rocha et al., 2019; Schaeffer et al., 2016).

65 In this study we examine the spatial and temporal variability of nutrients from the continental shelf to the off-shore region
at $\sim 27^\circ$ S. We use 10-years of nutrient bottle data collected between 2012–2022 (Sloyan et al., 2016, 2024). We examine the
seasonality of the nutrients and the role of the position of the EAC, relative to the continental shelf and slope, in influencing
the distribution of nutrients in the upper water column and find that there is a seasonal increase in nutrient concentrations in
the upper water column (0–200 m) in the Austral spring (September–November) and autumn (March–May), and a minimum in
70 winter (June–August). It is also clear that the nutrient concentrations in the upper water column are influenced by the bimodal
distribution of the EAC jet position. As the position of the EAC jet shifts longitudinally, it can be broadly categorised into two
modes: the inshore mode and offshore mode. When the EAC jet is in its inshore mode — jet located on the continental slope
— cooler, nutrient-rich waters are restricted to an area inshore of the EAC jet. The offshore EAC jet mode — EAC jet located
over the abyssal plain — is associated with a wider distribution of nutrient-rich waters that extends from the continental shelf,
75 across the slope and into the offshore waters of the adjacent abyssal plain. Our analysis highlights the important interactions
between nutrient concentrations and distribution and the highly variable EAC, which has implications for primary production,
fisheries, and the biological carbon pump. Understanding the dynamical implications of the EAC on nutrient distribution is
essential for elucidating the broader implications of the EAC’s role on marine ecosystems and fisheries. This long-term dataset
offers a valuable insight into the oceanography, biogeochemical cycling, and the EAC’s dynamical influence on surface and
80 mixed layer nutrient concentrations.

2 Methods

2.1 Data

2.1.1 The EAC Moorings

To capture the behaviour of the EAC in the intensification zone where it has a defined jet-like structure, a “picket-fence”
85 mooring array was established by CSIRO and the Australian Integrated Marine Observing System (IMOS) at approximately
 27° S, offshore of Brisbane, Australia (Sloyan et al., 2024). The mooring array was operational from 2012 to 2022, except
for a 22-month period between 2013 and 2015. The EAC mooring array extends from 153.5° E to 155.5° E, covering a depth
range of approximately 60 m to 5000 m (Figure 1; Sloyan et al. (2024)). The moorings were equipped with Acoustic Doppler
current profiling (ADCP) instruments that provided a vertical profile of horizontal current velocity and discrete temperature
90 and salinity instruments at various vertical intervals. The data used in this study is the daily mooring velocity data product

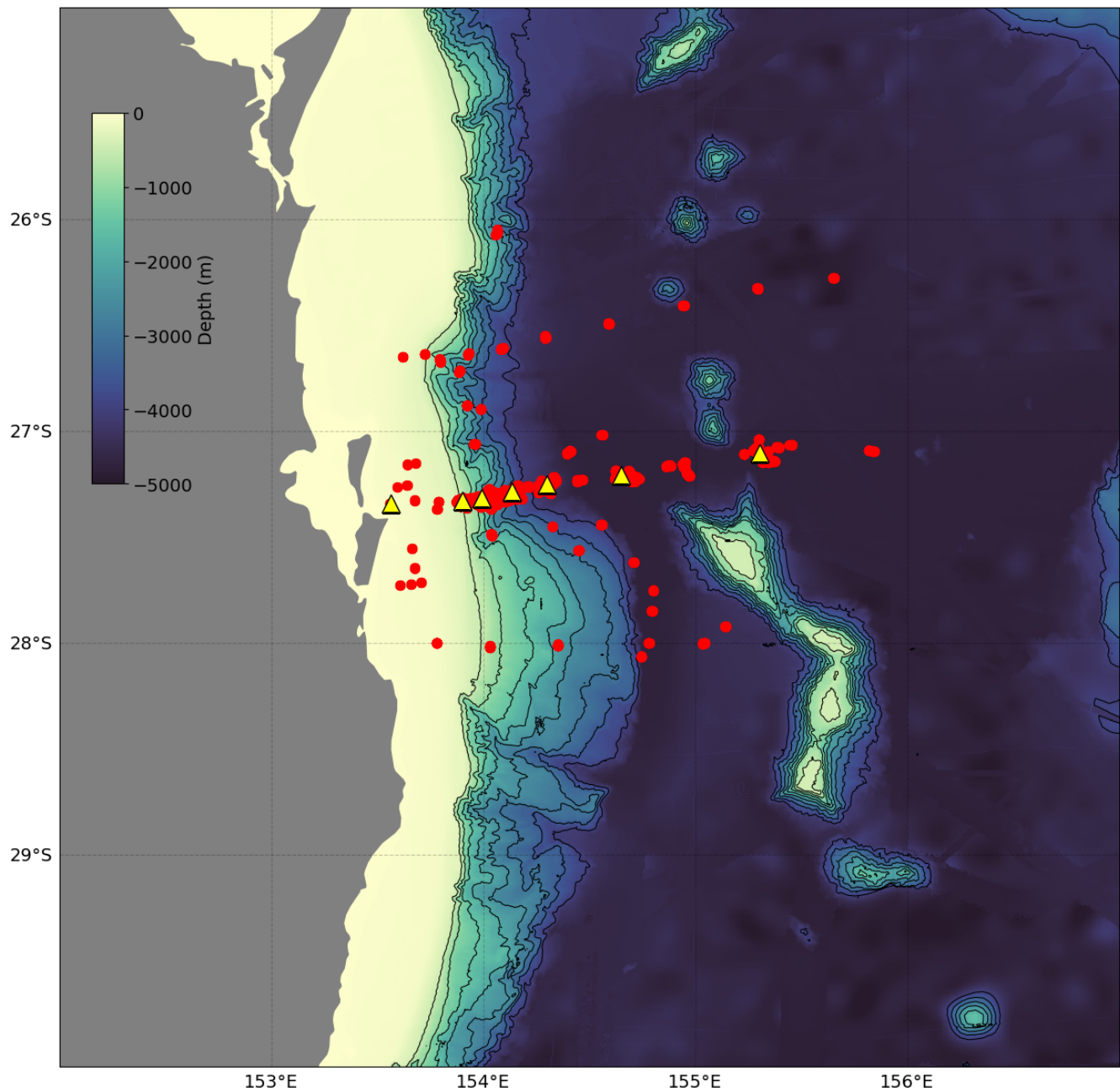


Figure 1. Location of CTD and hydrochemistry stations (red dots) and EAC array moorings (black triangles) used in this study. The bathymetric map of the study area is also shown. The contour interval (black line) is every 500 m from 50 m water depth.

with missing or bad velocities “filled” using a machine learning approach (<https://doi.org/10.25919/10h0-yf37> ; Sloyan et al. (2023, 2024)).



Table 1. List of voyages from which the CTD and nutrient data were used for this study. Including voyage ID, dates, research vessel and number of CTD casts deployed.

Voyage ID	Voyage Dates	Vessel	No. Deployments
SS2012_V01	20 th April – 29 th April 2012	Southern Surveyor	8
SS2013_V05	20 th August – 2 nd September 2013	Southern Surveyor	25
IN2015_V02	15 th May – 26 th May 2015	<i>RV Investigator</i>	16
IN2016_V04	30 th August – 23 rd September 2015	<i>RV Investigator</i>	3
IN2016_V06	28 th October – 13 th November 2016	<i>RV Investigator</i>	12
IN2018_V03	29 th April – 10 th May 2018	<i>RV Investigator</i>	13
IN201_V05	9 th September – 29 th September 2019	<i>RV Investigator</i>	25
IN2021_V03	7 th May – 2 nd June 2021	<i>RV Investigator</i>	16
IN2022_V06	14 th July – 28 th July 2022	<i>RV Investigator</i>	18

2.1.2 Conductivity, Temperature, Depth and Hydrochemical Data

For the assessment of the EAC's physical and biogeochemical properties, we utilize 136 Conductivity, Temperature, Depth (CTD) and Niskin bottle profiles collected during research voyages (Figure 1, Table 1). The CTD profiles provide measurements of temperature, salinity, and dissolved oxygen at 1 dbar pressure intervals. Nutrients were measured on water samples collected by Niskin bottles at discrete depths that span the entire water column. These water samples were analysed for nitrate, phosphate, and silicate (and nitrite and ammonia that are not used here). No voyages were conducted during Austral summer (November–March) in the region to avoid cyclone season, however all months from April to November were sampled, providing observations for Austral autumn, winter, and spring seasons over the 10-year period. All CTD data is available from the CSIRO Data Trawler (<https://www.cmar.csiro.au/data/trawler/>).

Although the CTD data are full depth (depths >4500 m over the abyssal plain), we use data from the upper 200 m of the water column, as this depth range span the EAC jet core (Sloyan et al., 2024). This depth range also includes a significant phytoplankton production, which is at a maximum in the Coral and Tasman Sea at a range of depths between 40–100 m depth (Ellwood et al., 2013). In the southwest Pacific plankton tend to be nitrate and phosphate limited (Ellwood et al., 2013; Ustick et al., 2021) as the southwest Pacific contains a low dissolved phosphorus region centred around 28° S (Martiny et al., 2019). Silicate is also limited in this region, although siliceous diatoms dominate the phytoplankton community (Ellwood et al., 2013; Eriksen et al., 2019).

2.2 Methods

We collate the 10-years of ship-based hydrographic data and analyse the physical (temperature and salinity) and biogeochemical (oxygen and nutrients) properties between 0–200 m across the longitudinal extent of the EAC mooring array. Mixed Layer depth (MLD) was calculated using density-based procedures developed by Holte and Talley (2009).

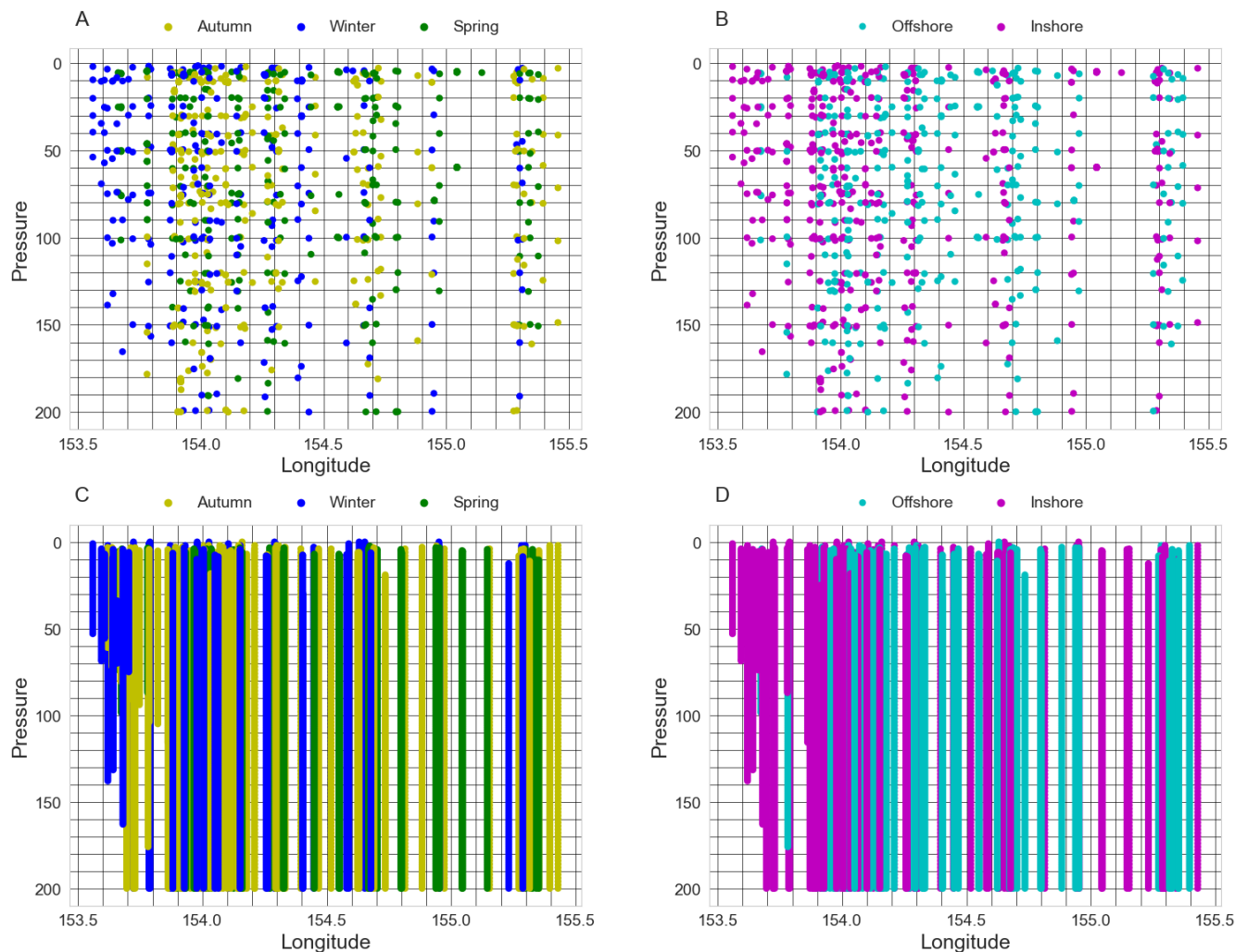


Figure 2. All hydrographic data points (coloured dots and lines) and grid (black lines) used for interpolated property section. Distribution of nutrient data (a) grouped by season, and (b) EAC mode, and distribution of CTD data (c) grouped by seasons, and (d) and EAC mode.

The hydrographic data are grouped by season and by mode position of the EAC jet (Figure 2). For each day that a CTD station was occupied, we classified the EAC into an “inshore mode” or an “offshore mode” using a qualitative description of the velocity profiles, based on the meridional velocities and position of the EAC core from the mooring data. The inshore mode was defined when the strongest southward flow was between 40–100 m (approximately the EAC core) and adjacent to, or “attached” to the continental slope, westward of approximately 154.2° E. The inshore mode is similar to the climatological position of the EAC in this area (Figure 3). The offshore mode was defined when the strongest southward flow was “detached” from the continental slope, eastward of approximately 154.2° E and found over the abyssal plain or at the eastern edge of the



120 mooring array. The inshore and offshore modes approximately match the mode 1 and mode 2 velocities from Sloyan et al. (2016).

After grouping the hydrographic profiles into season and EAC jet position we interpolate the temperature, salinity, oxygen and nutrient data to a 10 dbar vertical and 0.1° longitude grid to produce property sections for each season and EAC mode (Figures 2, 4, and 6). To test for statistical significance, a Monte Carlo simulation was run. For each parameter, a random subset
125 of data points were selected and used to make an interpolated pressure-longitude transect. This was repeated 1000 times and sections were constructed by selecting only the $<5^{\text{th}}$ and $>95^{\text{th}}$ percentile observations for each grid cell from the Monte Carlo. Stippling was added to all seasonal and mode sections for areas of statistical significance at the 95% confidence interval.

3 Results

3.1 Seasonality

130 We will first focus on the seasonal variability of the physical and biogeochemical variables in the EAC during austral autumn (March–May), winter (June–August), and spring (September–November).

The upper 200 m of the water column shows temperature ranges between ~ 15 – 25°C , salinity ranges between ~ 35 – 35.8 and oxygen ranges between 160–230 $\mu\text{mol/L}$ for all seasons (Figure 4). In general, water is warmest, freshest and most oxygenated in the upper ~ 50 m and becomes cooler and reduced in oxygen with depth. The surface waters (0–100 m) are warmest in autumn,
135 cooler during the winter period, and begin to rise in temperature during spring. During both austral autumn and spring, there is a sharper gradient in both temperature, salinity, and oxygen between the surface and 200 m depth across the transect compared to winter. Oxygen concentrations above the mixed layer are lowest in autumn, increase in winter, and reach a maximum in spring. Below the mixed layer, the lowest oxygen concentrations are found near the western boundary and highest oxygen concentrations along the eastern edge of the section. Salinity is highly variable, with the near surface (above the mixed layer)
140 having a minimum in autumn, increasing through winter, and reaching a maximum in spring. The subsurface salinity (50–150 m) has highest values in spring. The winter seasonal changes in temperature, salinity and oxygen have little statistical significance from the mean state, however, the seasonal extremes of warm, fresh, oxygen poor waters in autumn, and cool, saline, more oxygenated waters in spring are statistically significant, particularly in the near-surface.

There was a slight seasonal cycle in MLD. There was a moderate mixed layer in Autumn (mean MLD of 36.08 m, interquar-
145 tile range (IQR) of 21.75–47.75 m, and 90^{th} percentile 57.75 m), followed by a deepening in winter (mean MLD of 43.65 m, IQR of 16.50–62.75 m and 90^{th} percentile of 85.80 m), and shoaling in spring (mean MLD of 25.40 m, IQR of 15.13–29.38 m and 90^{th} percentile of 41.35 m).

The Temperature, Salinity, Oxygen (TS-O) diagrams show that the surface waters ($\rho_\theta < 26.5$) are warmer with slightly lower salinity in autumn, cooling and freshening in winter, and increasing in temperature and salinity again in spring (Figure 5).
150 Surface waters are oxygen-rich, with oxygen decreasing in the subsurface waters. There is a slight increase in oxygen in the surface waters in winter and spring, likely due to slight cooling in the temperature. All seasons show anomalous low oxygen concentration within the surface layer, these are particularly evident in Autumn (Figure 5).

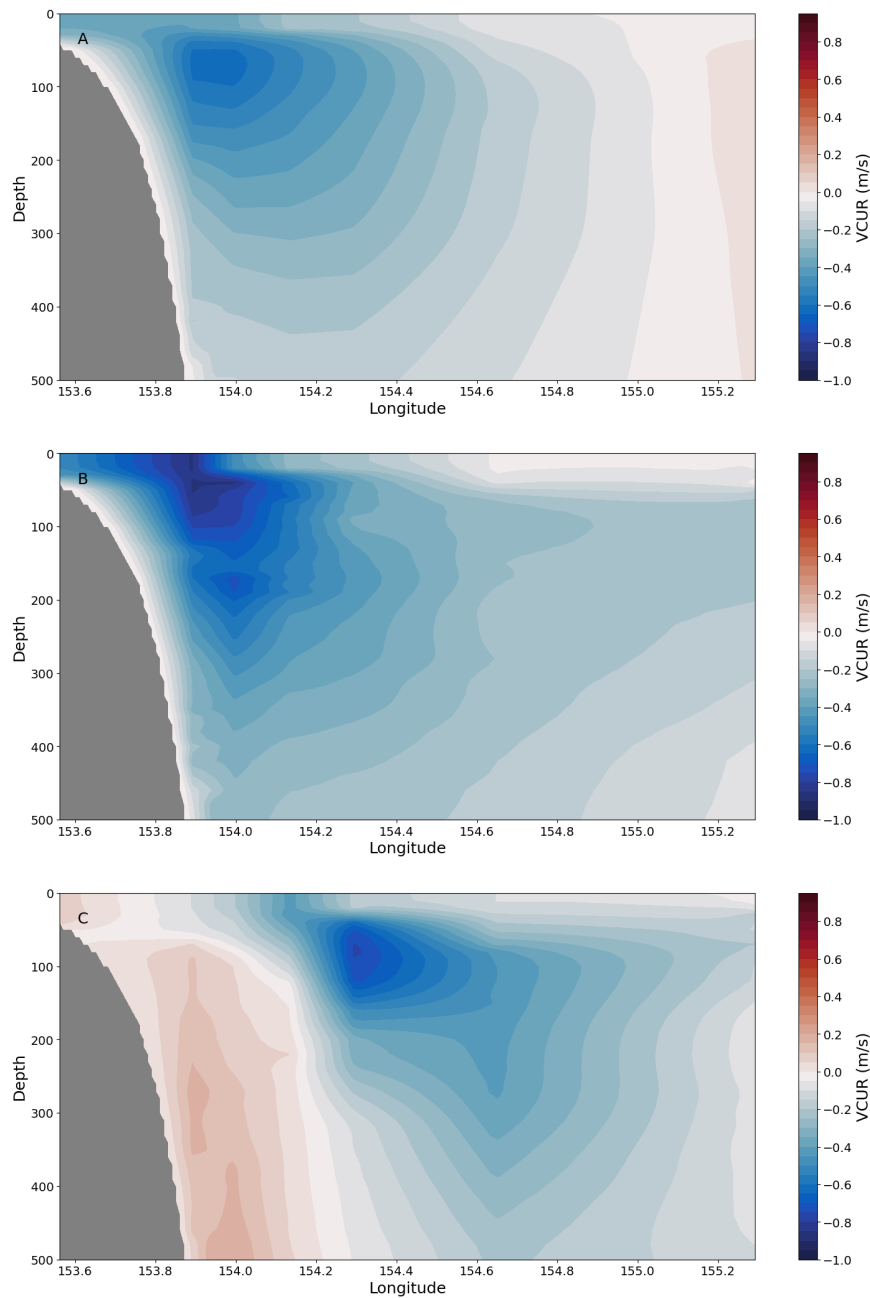


Figure 3. Meridional velocity (m/s) from the daily EAC mooring data product for (a) mean over all days with a CTD station, (b) a one-day mean example of the EAC jet inshore mode, and (c) a one-day mean example of the EAC jet offshore mode. Velocity is plotted for the upper 500 m of the water column.

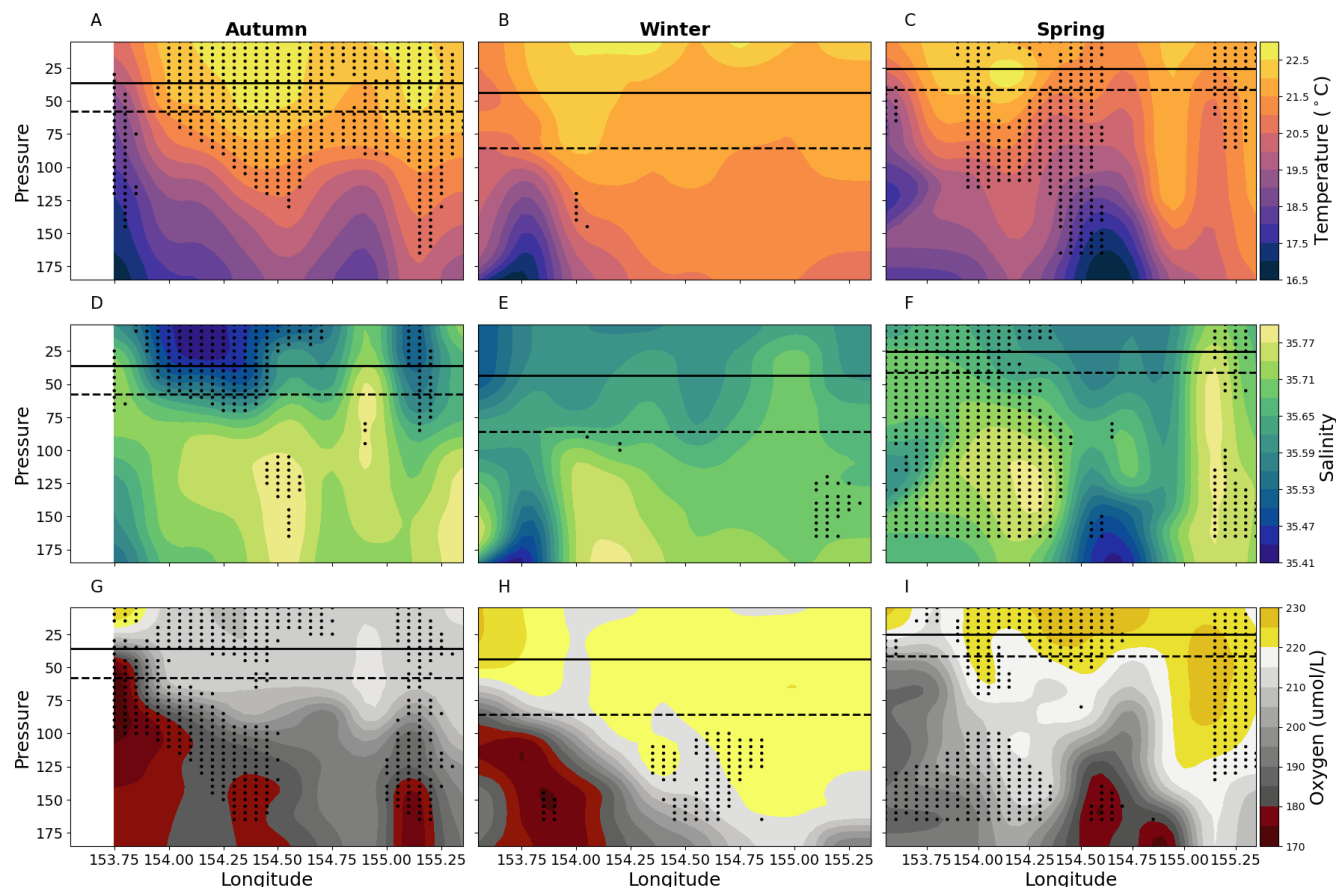


Figure 4. Vertical sections of ((a), (b), (c)) temperature ($^{\circ}\text{C}$), ((d), (e), (f)) salinity, and ((g), (h), (i)) oxygen ($\mu\text{mol/L}$) for the upper 200 m compiled from the 10 years (2012–2022) of data for austral autumn (March, April, May, left column), winter (June, July, August, middle column) and spring (September, October, November, right column). Solid lines shows mean MLD and dashed lines show the 90th percentile MLD averaged across longitude. Stippling indicates statistically significant departures from the average obtained using all data following the procedure described in the Data and Methods section.

Nutrient concentrations are generally low at the surface (0–50 m) and increase with depth (Figure 6). The ratio of nitrate to phosphate for 0–100 m and 100–200 m is 13.19 and 15.11, respectively. These values approximately agree with the Redfield ratio, particularly between 100–200 m. There is evidence for a subtle seasonal cycle in nutrients when grouping together all data in the upper 200 m of the water column, although at these depths the changes between seasons are subtle (Figure 8 (a)–(c)). There is little change to nitrate, although there is an increased number of observations with high concentration in autumn compared to winter and spring. Phosphate experiences a slight increase each season from autumn through to spring. Silicate has the largest mean in winter and lowest in spring.

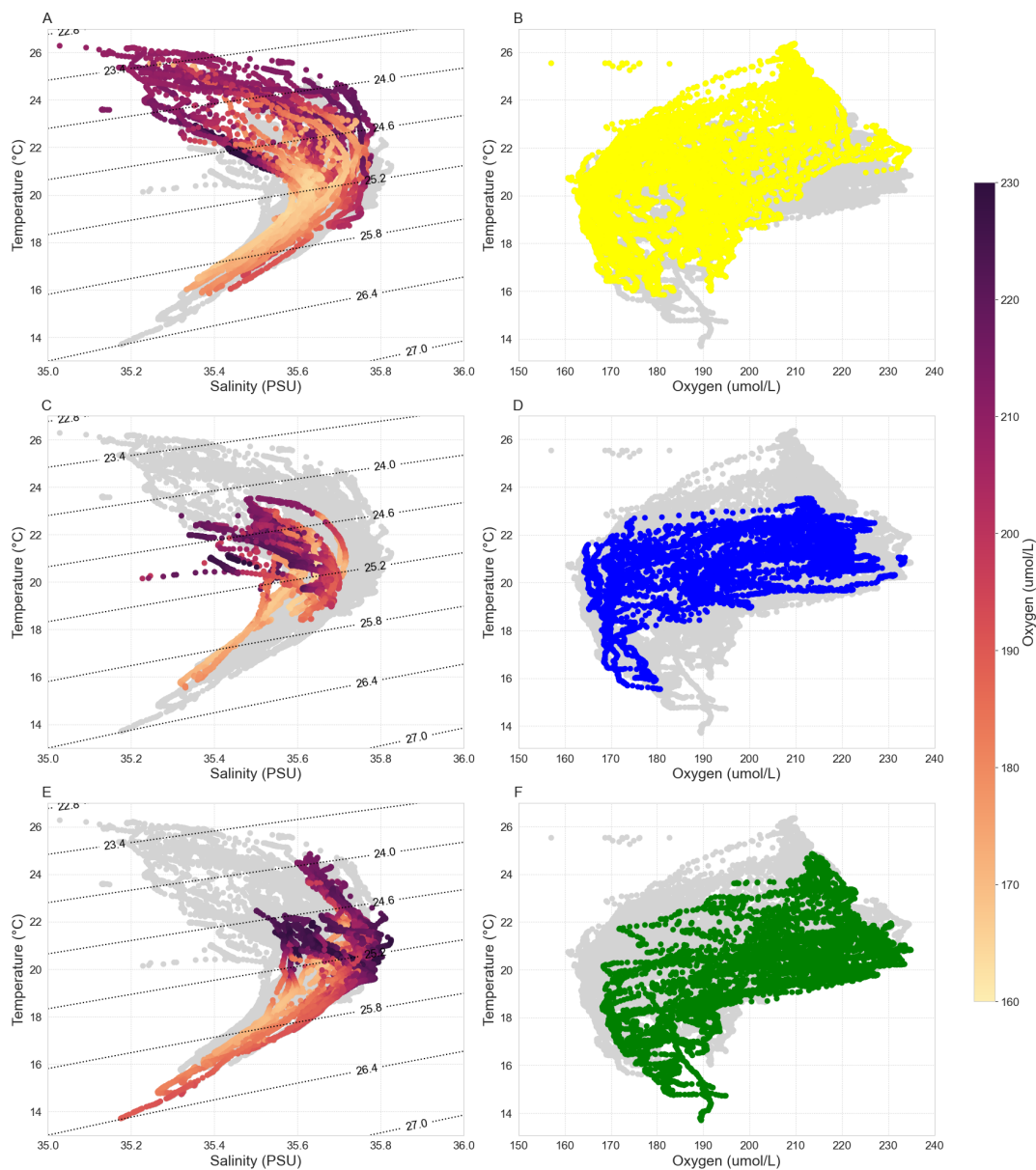


Figure 5. T-S-O diagrams for austral (a) autumn, (c) winter, and (e) spring with oxygen concentrations coloured. T-O diagrams for austral (b) autumn (yellow), (d) winter (blue) and (f) spring (green). All CTD stations are shown in grey in each figure and potential density isopycnals (kg m^{-3}) are shown in light grey on T-S-O diagrams.

160 The nutrients also exhibit a seasonal change with the longitude. The western edge of the section (westward of approximately 154°E) has a similar distribution of nutrients throughout the water column during autumn and winter and a slight decrease in nutrient concentration during spring (Figure 6). The eastern section of the transect, particularly eastward of $\sim 154.5^\circ \text{E}$, surface

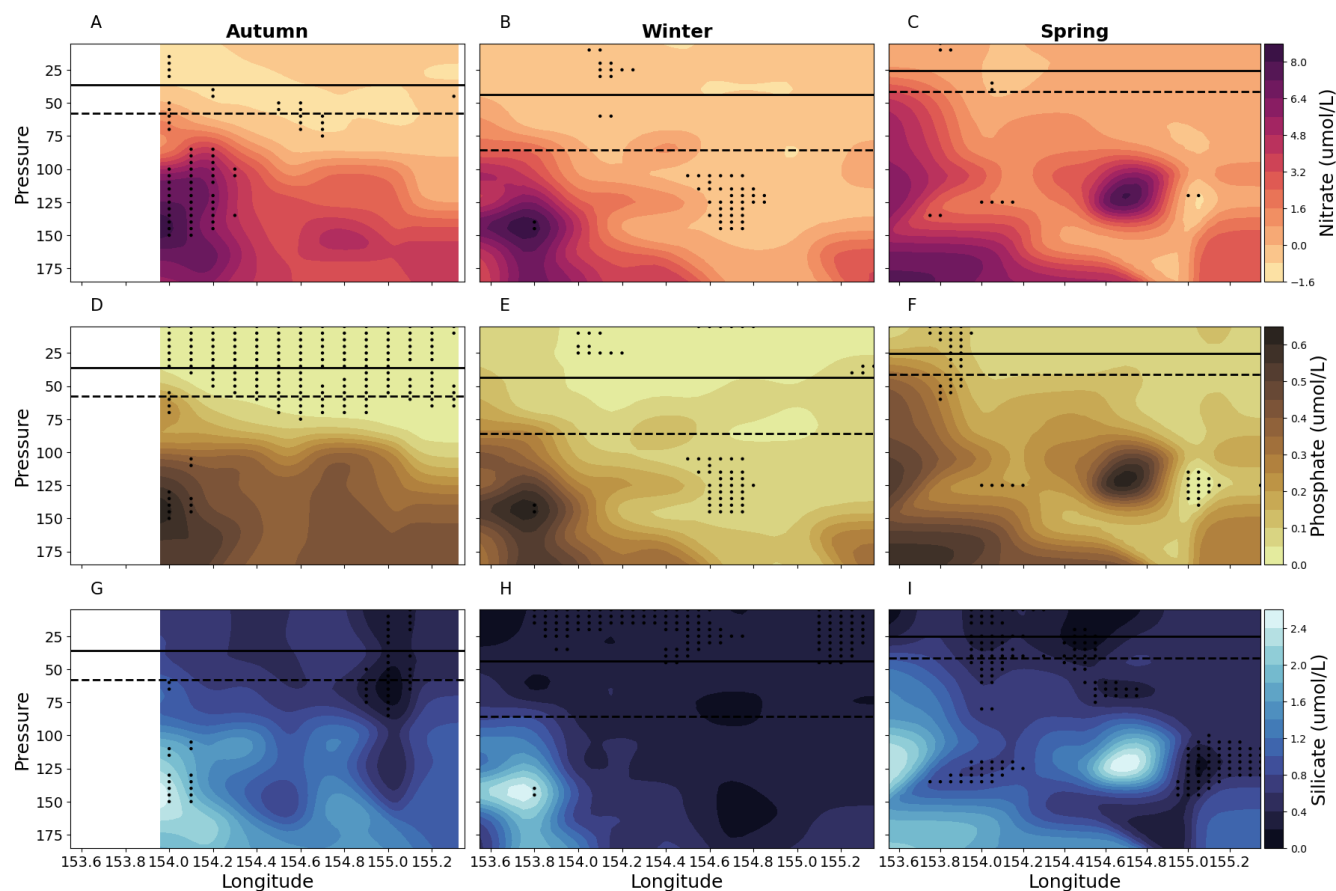


Figure 6. Vertical sections of ((a), (b), (c)) Nitrate ($\mu\text{mol/L}$), ((d), (e), (f)) Phosphate ($\mu\text{mol/L}$), and ((g), (h), (i)) Silicate ($\mu\text{mol/L}$) for the upper 200 m compiled from the 10-years (2012–2022) of data for austral autumn (March, April, May, left column), winter (June, July, August, middle column) and spring (September, October, November, right column). Solid lines shows mean MLD and dashed lines show the 90th percentile MLD averaged across longitude. Stippling indicates statistically significant departures from the average obtained using all data following the procedure described in the Data and Methods section.

waters between 50–200 m are more nutrient-rich during autumn, with reduced nutrient concentration during winter, and show an increase in nutrient concentration again during spring, although with more variability (Figure 6).

165 3.2 Response of the ocean environment to EAC variability

Here, we present the physical and biogeochemical characteristics sorted by EAC inshore or offshore mode. The inshore mode (Figure 3 (b) approximately follows the climatological position of the EAC, where meridional flow between 40–100 m is approximately $>0.4 \text{ m/s}$ in the poleward/southward direction and sits on to the continental slope, with the majority of the core sitting westward of 154.2° E . The inshore mode has southward velocity over the continental slope and northward velocity



Table 2. Number of days sampled in each season and mode. The percentage of days categorised in each mode for every season is shown in brackets, as well as total percentage number of days sampled in each mode and season.

Mode	Autumn	Winter	Spring	Total
Inshore	16 (38%)	17 (81%)	27 (64%)	60 (57%)
Offshore	26 (62%)	4 (19%)	15 (36%)	45 (43%)
Total	42 (40%)	21 (20%)	42 (40%)	105

170 further offshore at the eastern edge of the mooring array. In contrast, the EAC “offshore” mode (Figure 3 (c)) has an EAC jet that is displaced eastward from the continental slope and found to the east of $\sim 154.3^\circ$ E. In this “offshore” mode there is evidence for northward flow occurring inshore at depths below ~ 100 m. Both the inshore mode and the offshore mode occurred during all the seasons sampled, however, winter was dominated by inshore mode, whereas autumn and spring had a more even distribution of both modes (Table 2).

175 Similarly to the seasonally grouped sections, sections grouped into EAC jet “inshore” or “offshore” mode the warmest, freshest and most oxygenated water is found in the upper ~ 50 m and sections cool and have reduced in oxygen concentrations with depth (Figure 7). As mentioned the velocity profile of the inshore mode is similar to the climatological mean velocity profile of the EAC, thus, there is few significant changes to the properties of the water column. The offshore mode is cooler and more oxygenated than the inshore mode across most of the section. However, for the western portion below the mixed
 180 layer we find that the off-shore mode is warmer, more saline, and more oxygenated than the corresponding locations of the inshore mode. These offshore mode property differences are generally significant for the portion of the section that is west of the EAC core. There was no difference in mean MLD between the two modes (35.77 m vs 34.61 m), or in variability of MLD (IQR of 17.75–48.50 m vs 15.38–48.75 m). The 90th percentiles were 63.00 m vs 65.10 m.

The TS-O diagram (not shown) reveal little discernible difference between the two modes. In general, the surface waters are
 185 more oxygen-rich with oxygen decreasing in the subsurface waters. The two modes have a similar temperature and oxygen ranges.

When considering changes in nutrient concentrations for all data from across the top 200 m of the water column across all longitudes combined, there is not a clear change in nutrient concentrations between the two modes (Figure 8 d–f). Each mode has similar range and distribution of nutrient concentration with depth for all three nutrients sampled. However, the differences
 190 in nutrient concentrations become more clear when considering the effect of depth and longitude (Figure 9).

The nutrient sections based on EAC jet location show that generally nutrient poor water is found above the mixed layer during the inshore mode, and the highest nutrient concentrations occur at the western edge of the section at approximately 150 m depth (Figure 9). For the offshore mode, waters are generally more nutrient-rich. Whilst there are not widespread statistically significant increases in nutrient concentrations between the two modes and the mean state, there is evidence for an
 195 increase in the concentrations of nitrate and phosphate above the mixed layer during the offshore mode when compared to the inshore mode.

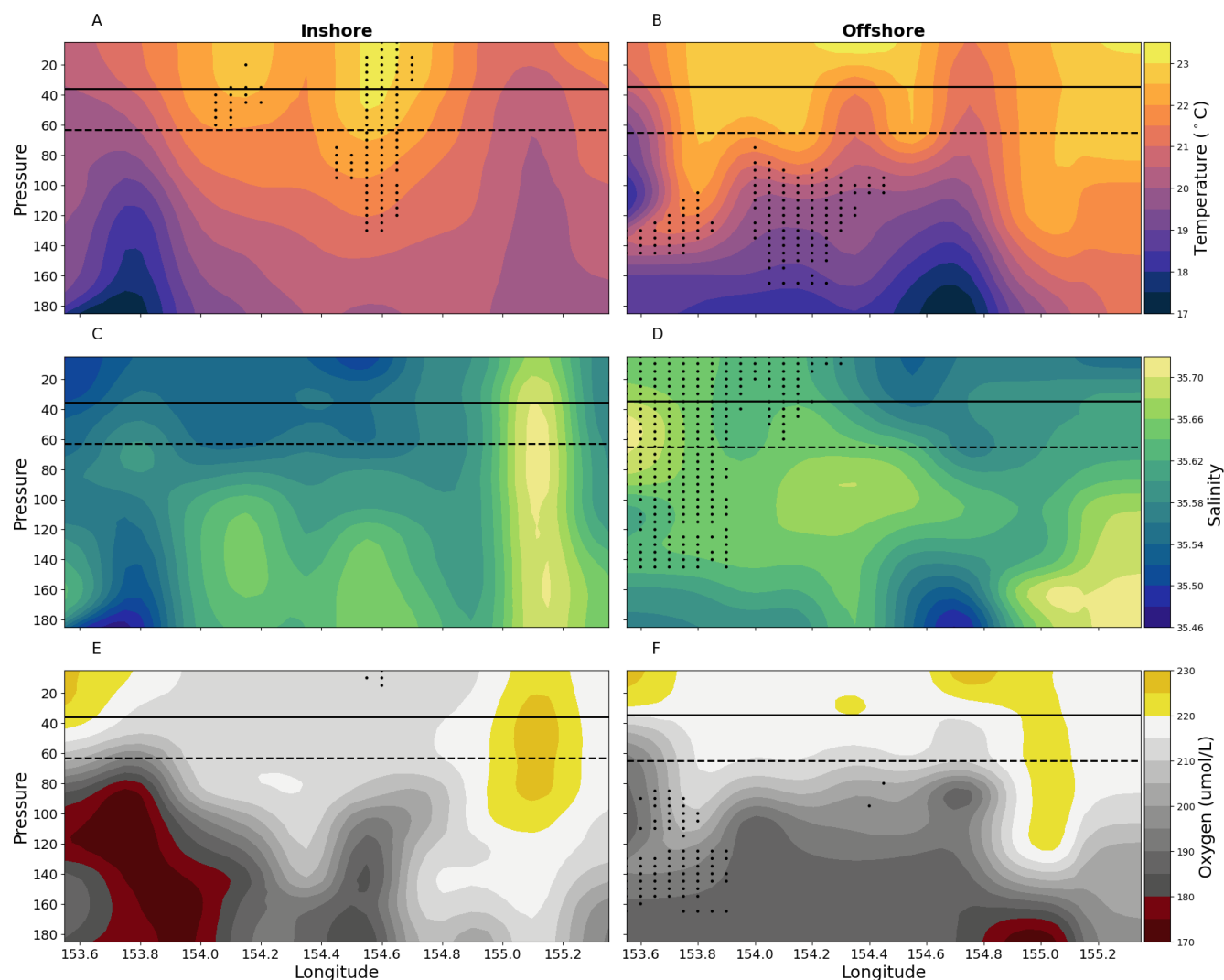


Figure 7. Vertical sections of (a, b) temperature ($^{\circ}\text{C}$), (c, d) salinity, and (e, f) oxygen ($\mu\text{mol/L}$) for the upper 200 m compiled from the 10 years (2012–2022) of data for the two EAC jet modes — inshore mode (left column), and offshore mode (right column). Solid lines shows mean MLD and dashed lines show the 90th percentile MLD averaged across longitude. Stippling indicates statistically significant departures from the average obtained using all data following the procedure described in the Data and Methods section.

4 Discussion

The results suggest that nitrate, phosphate, and silicate peak in concentration in autumn and spring below the mixed layer, but these are associated with different oxygen concentrations. There is a low-oxygen high nutrient peak in autumn and a higher-
 200 oxygen nutrient peak in early spring. Previous observations from coastal sites have found a spring peak in nutrients at 29° S (Everett et al., 2014) and also at the North Stradbroke Island National Reference Site (27° S; (Butler et al., 2020)). They

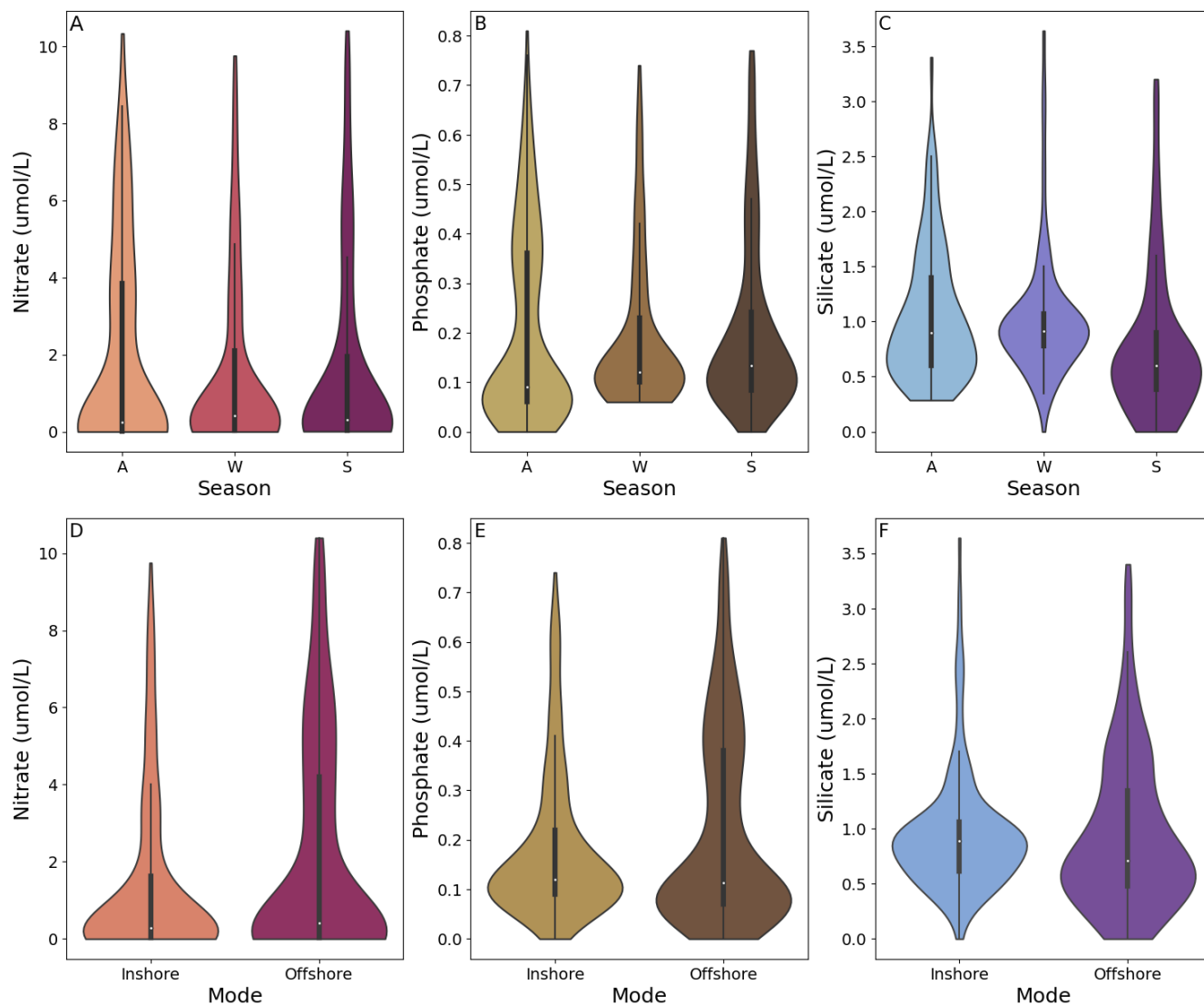


Figure 8. Violin plots of nutrient concentrations across (a, b, c) the three seasons (Austral autumn (A), winter (W), and spring (S) and (d, e, f) the two modes sampled.

also suggested an early winter minimum in silicate. Additionally, Rocha et al. (2019) found that the nutricline deepens by approximately 50 m during the summer, reducing availability of nutrients to the surface waters.

While we also find a seasonal nutrient signal, we show an interesting impact of the position of the EAC core relative to the continental shelf/slope. The different modes in the EAC jet did not alter the average properties of the water column, but they did impact the vertical distribution of nutrients in the upper water column, and longitudinally along the transect line. For both modes, we see evidence of upwelling, with of cooler, fresher, oxygen poor, and nutrient-rich water being found closer

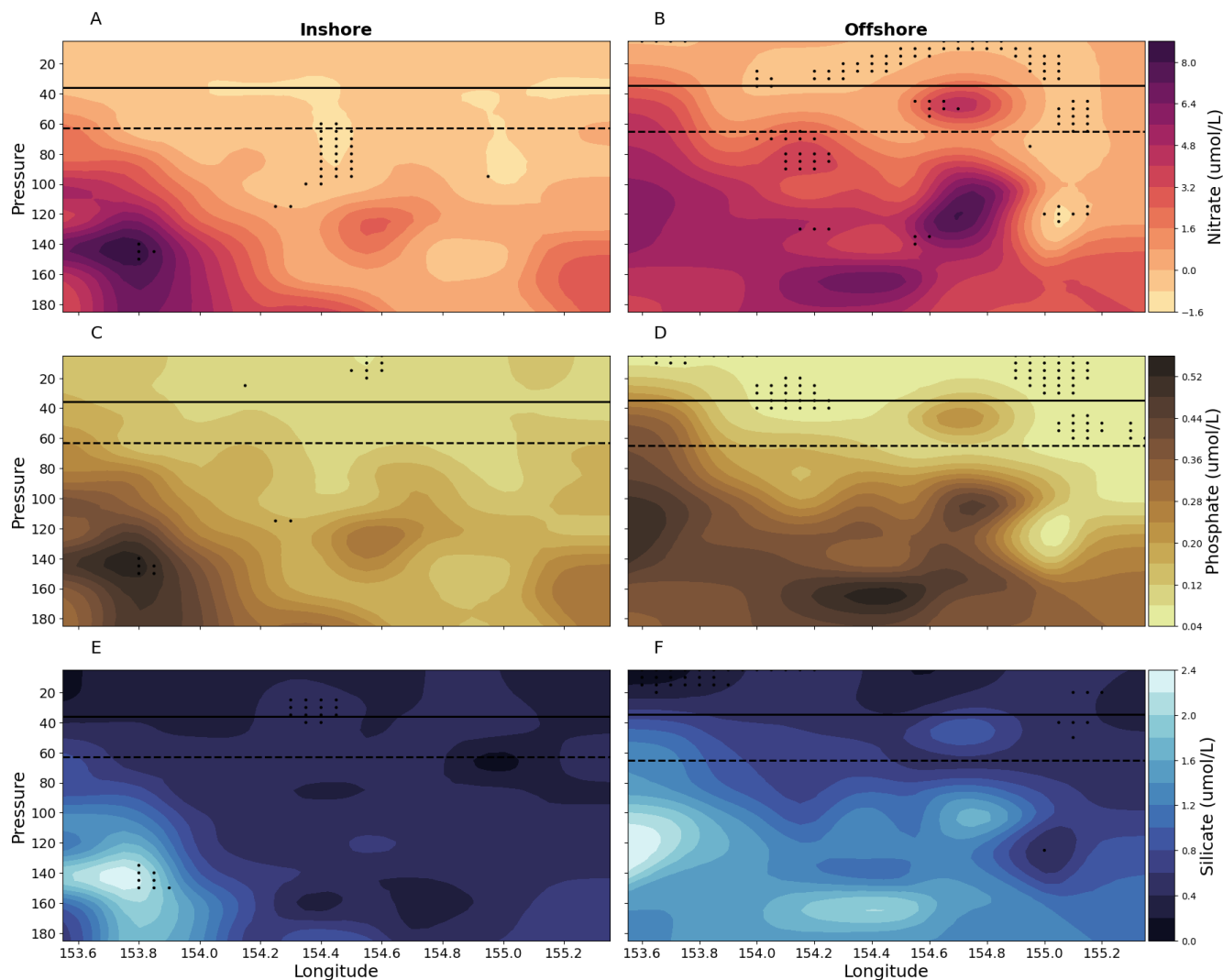


Figure 9. Vertical sections of (a, b) Nitrate (umol/L), (c, d) Phosphate (umol/L), and (e, f) Silicate (umol/L) for the upper 200 m compiled from the 10-years (2012–2022) of data for the two EAC jet modes — inshore mode (left column), and offshore mode (right column). Solid lines shows mean MLD and dashed lines show the 90th percentile MLD averaged across longitude. Stippling indicates statistically significant departures from the average obtained using all data following the procedure described in the Data and Methods section.

to the surface. For the inshore mode, this upwelling signature occurs on the western (inshore) edge of the property sections (west of 154° E), whereas for the offshore mode, the upwelling signature is found off-shore at ~154.7° E. Additionally, the MLD is similar between the two modes, meaning that upwelling in the offshore mode results in higher concentrations of nutrients entering the mixed layer during the offshore mode compared to the inshore mode. The effect of the EAC core location

210



highlights a potential mechanism for episodic nutrient supply to the surface layer, as both the inshore mode and offshore mode were observed in all three seasons.

The upwelling that occurs in the two EAC jet modes may be connected to different drivers. The encroachment of the EAC towards the continental shelf can cause upwelling along the slope (Schaeffer et al., 2013). Additionally, increasing EAC speeds has previously been linked to upwelling (Archer et al., 2017a; Oke and Middleton, 2001; Roughan and Middleton, 2002). As such, the inshore mode of the EAC – characterised by high speeds and a position close to the continental shelf – may still experience some upwelling of nutrient rich waters, however this upwelling will be limited to the slope/shelf area. This is compared to the offshore mode, where upwelling could be linked to eddy interactions and sub-mesoscale circulations (*e.g.*, Roughan et al., 2017; Roughan and Middleton, 2004; Suthers et al., 2011), meaning upwelling can occur over a broader longitudinal range.

The drivers of the shift in the position of the EAC core are yet to be determined. Early studies implied seasonality plays a role in jet meandering (Ridgway and Godfrey, 1997), while more recent studies found seasonality plays no role in the core position (Archer et al., 2017a). It may be related to the energy of the EAC system, as higher energy jet separates further north and creates larger scale meandering (Li et al., 2021). However, none of the previous studies have been able to attribute EAC wavering or meandering to one clear cause (Archer et al., 2017a; Bowen et al., 2005; Sloyan et al., 2016). Despite this, the effects of mesoscale eddy interactions are heavily implicated, as there are strong interactions between eddies and the mean flow path of the EAC (Li and Roughan, 2023).

Similar variability has been observed in other WBCs, for example the Gulf Stream (Mao et al., 2023), the Florida Current (Archer et al., 2018), Agulhas Current (Goschen et al., 2015), and the Brazil Current (Da Silveira et al., 2008). The Kuroshio Current also experiences variability in its core position and strength, and experiences meandering and interactions with bathymetry and mesoscale eddies (Ebuchi and Hanawa, 2003; Kawabe, 2005, 1995; Waseda et al., 2003). South of Japan, the Kuroshio Current follows three main flow paths, flow following the coastline, flow that separates from the coast resulting in offshore flow, and finally, a large meander mode that greatly changes the current position (Kawabe, 1985, 1995). Additionally, in the upstream region of the Kuroshio near Taiwan, it has been found that increased speed of the Kuroshio current causes an increased uplift of nutrients onshore (Chen et al., 2022). This is similar to the inshore position of the EAC, where there are faster speeds near the continental shelf and upwelling of nutrients along the slope. Additionally, periods where the Kuroshio sits closer to the coast, it interacts with bathymetry which causes strong vertical mixing and uplift of nutrients to the continental shelf (Durán Gómez and Nagai, 2022). The Florida Current is upstream of the Gulf Stream, and has a very similar jet structure to the EAC when considering jet coordinates (Archer et al., 2018), and exhibits a similar meandering behaviour, with meanders occurring on a time-scale of 3–30 days (Archer et al., 2017b). Mesoscale variability in the Florida Current is mainly linked to two mechanisms, frontal eddies and current meandering, both of which are linked to the upwelling of cool, nutrient rich waters between the shelf break and the offshore meander (Fiechter and Mooers, 2007; Kourafalou and Kang, 2012). Upwelling has also been linked to the movement of jet meanders in the Agulhas Current, with upwelling occurring when the current shifts onto the continental shelf, or shifts offshore (Goschen et al., 2015). It is clear that meandering of the current upstream of the separation point is not unique to the EAC, and the dynamics of WBC meandering, including the identification of upwelling, has



been observed in several WBC systems. However, we still lack a detailed understanding of the impact of current meandering on the biogeochemistry of the upper ocean and continental shelf.

250 Previous work has found existing relationships between ENSO and EAC transport (Holbrook et al., 2011). Though we do not present the results here, we found that the position of the EAC and El Niño Southern Oscillation (ENSO) Index (SOI), using a linear model, to be highly correlated. Periods of El Niño (positive SOI) showed increased occurrences of the EAC offshore mode. However, a full analysis of the connection between ENSO and EAC current position could not be conducted due to the limited duration of the dataset. It is worth noting that even when considering other long datasets, only a handful of strong ENSO events have occurred in conjunction with comprehensive oceanographic and mooring data, therefore there is
255 limited data to robustly test these hypotheses. So, while there is some evidence for a link between EAC meandering and ENSO, longer timeseries data is needed to understand the mechanisms of such a connection.

The Southwest Pacific surface waters are oligotrophic, and plankton in this area are nitrate and phosphate limited (Ellwood et al., 2013; Ustick et al., 2021). The upwelling of nutrient rich waters can cause plankton blooms (Silsbe and Malkin, 2016) and has implications for greater ecosystems function (Brander et al., 2003; Hays et al., 2005; McGillicuddy Jr, 2016; Richardson
260 and Schoeman, 2004). Whilst we have observed mechanisms which lead to an increase of nutrients in the upper water column, exploring biological responses to such nutrient changes is out of the scope of this paper. Future work should explore measurements of the deep chlorophyll-a maximum or the plankton communities observed during these research voyages to determine the productivity response to nutrient upwelling. The improved understanding of biogeochemical dynamics and the associated plankton response will improve our ability to understand how marine ecosystems may respond to current meandering in the
265 EAC system.

5 Conclusions

This study systematically assesses the nutrient variability in the EAC intensification region, and is one of the few studies focusing on waters beyond the coastal and shelf environment. We find seasonal variability in the temperature, salinity, oxygen, and nutrients of the EAC, and importantly we identify the influence of EAC jet meandering on the location of the upwelled
270 nutrients. Furthermore, we categorized the EAC into two distinct modes based on the position of the current relative to the continental shelf and slope — the inshore and offshore modes. The offshore mode, when the EAC jet sits over the abyssal plain, exhibits nutrient-enriched waters and extending further offshore. Meanwhile the inshore mode shows upwelling of nutrients along the edge of the continental shelf. Understanding what drives the position of the EAC and the nutrient dynamics contributes to our knowledge of the EAC's role in supporting and shaping the biological communities and productivity within
275 this region.

Author contributions. BS and CC designed and lead voyages and supplied data. MJ and CC designed and undertook analysis. MJ prepared manuscript with critical comment and editing from all authors.

<https://doi.org/10.5194/egusphere-2024-2265>

Preprint. Discussion started: 30 July 2024

© Author(s) 2024. CC BY 4.0 License.



Competing interests. At least one of the (co-)authors is a member of the editorial board of Ocean Science.

Acknowledgements. We acknowledge the use of the CSIRO Marine National Facility (<https://ror.org/01mae9353>) and grant of sea time on
280 RV Investigator in undertaking this research. The authors would also like to acknowledge the hydro-chemistry teams from all voyages that
undertook nutrient analysis.



References

- Archer, M., Keating, S., Roughan, M., Johns, W., Lumpkin, R., Beron-Vera, F., and Shay, L.: The kinematic similarity of two western boundary currents revealed by sustained high-resolution observations, *Geophysical research letters*, 45, 6176–6185, 2018.
- 285 Archer, M. R., Roughan, M., Keating, S. R., and Schaeffer, A.: On the variability of the East Australian Current: Jet structure, meandering, and influence on shelf circulation, *Journal of Geophysical Research: Oceans*, 122, 8464–8481, 2017a.
- Archer, M. R., Shay, L. K., and Johns, W. E.: The surface velocity structure of the Florida Current in a jet coordinate frame, *Journal of Geophysical Research: Oceans*, 122, 9189–9208, 2017b.
- Blackburn, S. and Cresswell, G.: A coccolithophorid bloom in Jervis Bay, Australia, *Marine and Freshwater Research*, 44, 253–260, 1993.
- 290 Boland, F. and Church, J.: The East Australian Current 1978, *Deep Sea Research Part A. Oceanographic Research Papers*, 28, 937–957, 1981.
- Bowen, M. M., Wilkin, J. L., and Emery, W. J.: Variability and forcing of the East Australian Current, *Journal of Geophysical Research: Oceans*, 110, 2005.
- Brander, K., Dickson, R., and Edwards, M.: Use of Continuous Plankton Recorder information in support of marine management: applications in fisheries, environmental protection, and in the study of ecosystem response to environmental change, *Progress in Oceanography*, 58, 175–191, 2003.
- 295 Bull, C. Y. S., Kiss, A. E., Gupta, A. S., Jourdain, N. C., Argüeso, D., Di Luca, A., and Sérazin, G.: Regional versus remote atmosphere-ocean drivers of the rapid projected intensification of the East Australian Current, *Journal of Geophysical Research: Oceans*, 125, e2019JC015889, <https://doi.org/https://doi.org/10.1029/2019JC015889>, 2020.
- 300 Butler, E., Skuza, M., and Lønborg, C.: Spatial and temporal trends in concentrations of nutrients, 2020.
- Chen, C.-C., Lu, C.-Y., Jan, S., Hsieh, C.-h., and Chung, C.-C.: Effects of the coastal uplift on the Kuroshio ecosystem, Eastern Taiwan, the western boundary current of the North Pacific Ocean, *Frontiers in Marine Science*, 9, 796 187, 2022.
- Da Silveira, I., Lima, J., Schmidt, A., Ceccopieri, W., Sartori, A., Francisco, C., and Fontes, R.: Is the meander growth in the Brazil Current system off Southeast Brazil due to baroclinic instability?, *Dynamics of Atmospheres and Oceans*, 45, 187–207, 2008.
- 305 Durán Gómez, G. S. and Nagai, T.: Elevated Nutrient Supply Caused by the Approaching Kuroshio to the Southern Coast of Japan, *Frontiers in Marine Science*, 9, 842 155, 2022.
- Ebuchi, N. and Hanawa, K.: Influence of mesoscale eddies on variations of the Kuroshio path south of Japan, *Journal of oceanography*, 59, 25–36, 2003.
- Ellwood, M. J., Law, C. S., Hall, J., Woodward, E. M. S., Strzepek, R., Kuparinen, J., Thompson, K., Pickmere, S., Sutton, P., and Boyd, P. W.: Relationships between nutrient stocks and inventories and phytoplankton physiological status along an oligotrophic meridional transect in the Tasman Sea, *Deep Sea Research Part I: Oceanographic Research Papers*, 72, 102–120, 2013.
- 310 Eriksen, R. S., Davies, C. H., Bonham, P., Coman, F. E., Edgar, S., McEnulty, F. R., McLeod, D., Miller, M. J., Rochester, W., Slotwinski, A., et al.: Australia's long-term plankton observations: the integrated marine observing system national reference station network, *Frontiers in Marine Science*, p. 161, 2019.
- 315 Everett, J., Baird, M., and Suthers, I.: Three-dimensional structure of a swarm of the salp *Thalia democratica* within a cold-core eddy off southeast Australia, *Journal of Geophysical Research: Oceans*, 116, 2011.
- Everett, J. D., Baird, M. E., Roughan, M., Suthers, I. M., and Doblin, M. A.: Relative impact of seasonal and oceanographic drivers on surface chlorophyll a along a Western Boundary Current, *Progress in Oceanography*, 120, 340–351, 2014.



- Fiechter, J. and Mooers, C.: Primary production associated with the Florida Current along the East Florida Shelf: Weekly to seasonal variability from mesoscale-resolution biophysical simulations, *Journal of Geophysical Research: Oceans*, 112, 2007.
- 320 Figueira, W. F. and Booth, D. J.: Increasing ocean temperatures allow tropical fishes to survive overwinter in temperate waters, *Global Change Biology*, 16, 506–516, 2010.
- Ganachaud, A., Cravatte, S., Melet, A., Schiller, A., Holbrook, N., Sloyan, B., Widlansky, M., Bowen, M., Verron, J., Wiles, P., et al.: The Southwest Pacific Ocean circulation and climate experiment (SPICE), *Journal of Geophysical Research: Oceans*, 119, 7660–7686, 2014.
- 325 Gibbs, M. T., Middleton, J. H., and Marchesiello, P.: Baroclinic response of Sydney shelf waters to local wind and deep ocean forcing, *Journal of Physical Oceanography*, 28, 178–190, 1998.
- Godfrey, J., Cresswell, G., Golding, T., Pearce, A., and Boyd, R.: The separation of the East Australian Current, *Journal of Physical Oceanography*, 10, 430–440, 1980.
- Goschen, W., Bornman, T., Deyzel, S., and Schumann, E.: Coastal upwelling on the far eastern Agulhas Bank associated with large meanders
330 in the Agulhas Current, *Continental Shelf Research*, 101, 34–46, 2015.
- Hassler, C., Djajadikarta, J., Doblin, M., Everett, J., and Thompson, P.: Characterisation of water masses and phytoplankton nutrient limitation in the East Australian Current separation zone during spring 2008, *Deep Sea Research Part II: Topical Studies in Oceanography*, 58, 664–677, 2011.
- Hays, G. C., Richardson, A. J., and Robinson, C.: Climate change and marine plankton, *Trends in ecology & evolution*, 20, 337–344, 2005.
- 335 Holbrook, N. J., Goodwin, I. D., McGregor, S., Molina, E., and Power, S. B.: ENSO to multi-decadal time scale changes in East Australian Current transports and Fort Denison sea level: Oceanic Rossby waves as the connecting mechanism, *Deep Sea Research Part II: Topical Studies in Oceanography*, 58, 547–558, 2011.
- Holte, J. and Talley, L.: A new algorithm for finding mixed layer depths with applications to Argo data and Subantarctic Mode Water formation, *Journal of Atmospheric and Oceanic Technology*, 26, 1920–1939, 2009.
- 340 Kawabe, M.: Sea level variations at the Izu Islands and typical stable paths of the Kuroshio, *Journal of the Oceanographical Society of Japan*, 41, 307–326, 1985.
- Kawabe, M.: Variations of current path, velocity, and volume transport of the Kuroshio in relation with the large meander, *Journal of physical oceanography*, 25, 3103–3117, 1995.
- Kawabe, M.: Variations of the Kuroshio in the southern region of Japan: Conditions for large meander of the Kuroshio, *Journal of oceanography*, 61, 529–537, 2005.
- 345 Kessler, W. S. and Cravatte, S.: Mean circulation of the Coral Sea, *Journal of Geophysical Research: Oceans*, 118, 6385–6410, 2013.
- Kourafalou, V. H. and Kang, H.: Florida Current meandering and evolution of cyclonic eddies along the Florida Keys Reef Tract: Are they interconnected?, *Journal of Geophysical Research: Oceans*, 117, 2012.
- Li, J. and Roughan, M.: Energetics of Eddy–Mean Flow Interactions in the East Australian Current System, *Journal of Physical Oceanography*, 53, 595–612, 2023.
- 350 Li, J., Roughan, M., and Kerry, C.: Dynamics of interannual eddy kinetic energy modulations in a western boundary current, *Geophysical Research Letters*, 48, e2021GL094 115, 2021.
- Mao, S., He, R., Bane, J., Gawarkiewicz, G., and Todd, R. E.: A data-assimilative modeling investigation of Gulf Stream variability, *Deep Sea Research Part II: Topical Studies in Oceanography*, 211, 105 319, 2023.
- 355 Martiny, A. C., Lomas, M. W., Fu, W., Boyd, P. W., Chen, Y.-I. L., Cutter, G. A., Ellwood, M. J., Furuya, K., Hashihama, F., Kanda, J., et al.: Biogeochemical controls of surface ocean phosphate, *Science Advances*, 5, eaax0341, 2019.



- McGillicuddy Jr, D. J.: Mechanisms of physical-biological-biogeochemical interaction at the oceanic mesoscale, *Annual Review of Marine Science*, 8, 125–159, 2016.
- Nieblas, A.-E., Sloyan, B. M., Hobday, A. J., Coleman, R., and Richardson, A. J.: Variability of biological production in low wind-forced regional upwelling systems: A case study off southeastern Australia, *Limnology and Oceanography*, 54, 1548–1558, 2009.
- 360 Oke, P. R. and Middleton, J. H.: Topographically induced upwelling off eastern Australia, *Journal of Physical Oceanography*, 30, 512–531, 2000.
- Oke, P. R. and Middleton, J. H.: Nutrient enrichment off Port Stephens: The role of the East Australian Current, *Continental Shelf Research*, 21, 587–606, 2001.
- 365 Oke, P. R., Roughan, M., Cetina-Heredia, P., Pilo, G. S., Ridgway, K. R., Rykova, T., Archer, M. R., Coleman, R. C., Kerry, C. G., Rocha, C., et al.: Revisiting the circulation of the East Australian Current: Its path, separation, and eddy field, *Progress in Oceanography*, 176, 102–139, 2019.
- Olson, D. B.: Biophysical dynamics of western transition zones: A preliminary synthesis, *Fisheries Oceanography*, 10, 133–150, 2001.
- Richardson, A. J. and Schoeman, D. S.: Climate impact on plankton ecosystems in the Northeast Atlantic, *Science*, 305, 1609–1612, 2004.
- 370 Ridgway, K. and Dunn, J.: Mesoscale structure of the mean East Australian Current System and its relationship with topography, *Progress in oceanography*, 56, 189–222, 2003.
- Ridgway, K. and Godfrey, J.: Seasonal cycle of the East Australian Current, *Journal of Geophysical Research: Oceans*, 102, 22 921–22 936, 1997.
- Rocha, C., Edwards, C. A., Roughan, M., Cetina-Heredia, P., and Kerry, C.: A high-resolution biogeochemical model (ROMS 3.4+ bio_Fennel) of the East Australian Current System, *Geoscientific Model Development*, 12, 441–456, 2019.
- 375 Rochford, D.: Nutrient enrichment of east Australian coastal waters. II. Laurieton upwelling, *Marine and Freshwater Research*, 26, 233–243, 1975.
- Roughan, M. and Middleton, J. H.: A comparison of observed upwelling mechanisms off the east coast of Australia, *Continental Shelf Research*, 22, 2551–2572, 2002.
- 380 Roughan, M. and Middleton, J. H.: On the East Australian Current: Variability, encroachment, and upwelling, *Journal of Geophysical Research: Oceans*, 109, 2004.
- Roughan, M., Keating, S., Schaeffer, A., Cetina Heredia, P., Rocha, C., Griffin, D., Robertson, R., and Suthers, I.: A tale of two eddies: The biophysical characteristics of two contrasting cyclonic eddies in the East Australian Current System, *Journal of Geophysical Research: Oceans*, 122, 2494–2518, 2017.
- 385 Roughan, M., Cetina-Heredia, P., Ribbat, N., and Suthers, I. M.: Shelf transport pathways adjacent to the East Australian Current reveal sources of productivity for coastal reefs, *Frontiers in Marine Science*, 8, 789–687, 2022a.
- Roughan, M., Hemming, M., Schaeffer, A., Austin, T., Beggs, H., Chen, M., Feng, M., Galibert, G., Holden, C., Hughes, D., et al.: Multi-decadal ocean temperature time-series and climatologies from Australia’s long-term National Reference Stations, *Scientific Data*, 9, 157, 2022b.
- 390 Schaeffer, A., Roughan, M., and Morris, B. D.: Cross-shelf dynamics in a western boundary current regime: Implications for upwelling, *Journal of Physical Oceanography*, 43, 1042–1059, 2013.
- Schaeffer, A., Roughan, M., Jones, E. M., and White, D.: Physical and biogeochemical spatial scales of variability in the East Australian Current separation from shelf glider measurements, *Biogeosciences*, 13, 1967–1975, 2016.



- Silsbe, G. M. and Malkin, S. Y.: Where light and nutrients collide: The global distribution and activity of subsurface chlorophyll maximum layers, *Aquatic microbial ecology and biogeochemistry: A dual perspective*, pp. 141–152, 2016.
- 395 Sloyan, B. M. and O’Kane, T. J.: Drivers of decadal variability in the Tasman Sea, *Journal of Geophysical Research: Oceans*, 120, 3193–3210, <https://doi.org/https://doi.org/10.1002/2014JC010550>, 2015.
- Sloyan, B. M., Ridgway, K. R., and Cowley, R.: The East Australian Current and property transport at 27°S from 2012 to 2013, *Journal of Physical Oceanography*, 46, 993–1008, 2016.
- 400 Sloyan, B. M., hapman, C. C., Cowley, R., and A, C. A.: Application of machine learning techniques to ocean mooring time series data, *Journal of Atmospheric and Oceanic Technology*, 40, 241–260, 2023.
- Sloyan, B. M., Cowley, R., and Chapman, C. C.: East Australian Current velocity, temperature and salinity data products, *Scientific Data*, 11, 10, 2024.
- Suthers, I. M., Young, J. W., Baird, M. E., Roughan, M., Everett, J. D., Brassington, G. B., Byrne, M., Condie, S. A., Hartog, J. R., Hassler, C. S., et al.: The strengthening East Australian Current, its eddies and biological effects—an introduction and overview, 2011.
- 405 Suthers, I. M., Schaeffer, A., Archer, M., Roughan, M., Griffin, D. A., Chapman, C. C., Sloyan, B. M., and Everett, J. D.: Frontal eddies provide an oceanographic triad for favorable larval fish habitat, *Limnology and Oceanography*, 2023.
- Sutton, P. J. and Bowen, M.: Flows in the Tasman front south of Norfolk island, *Journal of Geophysical Research: Oceans*, 119, 3041–3053, 2014.
- 410 Tranter, D. J., Carpenter, D. J., and Leech, G. S.: The coastal enrichment effect of the East Australian Current eddy field, *Deep Sea Research Part A. Oceanographic Research Papers*, 33, 1705–1728, 1986.
- Ustick, L. J., Larkin, A. A., Garcia, C. A., Garcia, N. S., Brock, M. L., Lee, J. A., Wiseman, N. A., Moore, J. K., and Martiny, A. C.: Metagenomic analysis reveals global-scale patterns of ocean nutrient limitation, *Science*, 372, 287–291, 2021.
- Waseda, T., Mitsudera, H., Taguchi, B., and Yoshikawa, Y.: On the eddy–Kuroshio interaction: Meander formation process, *Journal of Geophysical Research: Oceans*, 108, 2003.
- 415